Available online at www.sciencedirect.com
SCIENCE DIRECT®
Nuclear Instruments and Methods in Physics Research B 232 (2005) 53–58
NIM B Beam Interactions with Materials & Atoms
www.elsevier.com/locate/nimb

Role of projectile charge state in convoy electron emission by fast protons colliding with LiF(0 0 1)

I. Aldazabal [a,*], M.S. Gravielle [b], J.E. Miraglia [b], A. Arnau [c], V.H. Ponce [d,e]

[a] *Departamento de Física de Materiales, Facultad de Químicas UPV/EHU, Apartado 1072, 20080 San Sebastián, Spain*
[b] *Instituto de Astronomía y Física del Espacio, Consejo Nacional de Investigaciones Científicas y Técnicas and Departamento de Física, Facultad de Ciencias Exactas y Naturales, Universidad de Buenos Aires, C.C. 67, Suc. 28, 1428 Buenos Aires, Argentina*
[c] *Centro Mixto CSIC-UPV/EHU, Apartado 1072, 20080 San Sebastián, Spain*
[d] *Donostia International Physics Center DIPC, San Sebastián, Spain*
[e] *Centro Atómico Bariloche, Bariloche, Argentina*

Available online 27 April 2005

Abstract

Target ionization and projectile ionization differential cross sections are used to calculate the electron emission spectra by fast proton impact on ionic crystal surfaces under grazing incidence conditions.

Both bare protons and neutral hydrogen species are considered. We use a planar potential approach to determine the projectile trajectory that later on allows us to calculate the charge state fractions. We show that, although the fraction of protons is significantly higher, the contribution from neutral hydrogen ionization has to be considered. The energy and angular dependence of the spectra is analyzed.

PACS: 34.50.Dy; 34.50.Fa; 79.20.Hx; 79.20.Rf; 34.20.−b

Keywords: Electron emission; Ion–surface collision; Convoy electrons; Charge state

1. Introduction

The spectrum of electrons emitted in ion–surface collision gives information about the electronic and atomic structure of the surface topmost atomic layer and has lately been object of study [1–5]. At high emission energies two structures appear, the so called *convoy* and *binary* peaks, already known from atomic collisions [6–8].

We study the projectile (*electron loss to the continuum* or *ELC*) and surface (*electron capture to the continuum* or *ECC*) electron contributions to the convoy peak. Low energy electrons emitted in all directions from projectile ionization are expected

* Corresponding author. Tel.: +34 943 01 5386; fax: +34 943 01 5270.
E-mail address: ialdazabal@sq.ehu.es (I. Aldazabal).

0168-583X/$ - see front matter
doi:10.1016/j.nimb.2005.03.024

to play a role comparable to high energy forward emitted electrons from target ionization.

The projectile trajectory is treated classically and for the electron emission we use a binary collision model within the impact parameter formalism [9–11] in first Born approximation for ELC electrons [12,13] and the continuum-distorted-wave-Eikonal-initial-state (CDW-EIS) approximation for ECC electrons [14–16].

2. Theoretical model

We consider a heavy projectile P of charge q and mass M_p in grazing incidence on a surface with a velocity $\vec{v} = (v_s, v_z)$, v_s and v_z being the velocity components parallel and perpendicular to the surface, respectively. The triple differential cross section (TDCS) for electron emission is obtained considering binary collisions between the projectile and the surface atoms. The surface is thus treated as a collection of atoms, each of them contributing in its own to the total emission cross section.

Being a grazing collision, we can approximate the trajectory as a succession of differential trajectories Δx in which the projectile velocity component perpendicular to the surface is considered negligible, i.e. the projectile moves at a constant distance from the surface $z(x)$ (see Fig. 1).

Under these assumptions we can study the collision with the straight-line version of the impact parameter approximation to obtain both the projectile and surface ionization cross sections.

Since target electrons are localized around atoms, only electrons of atoms situated in the top most layer contribute effectively to the electron emission process.

Then for a given height z over the surface, the emission probability per unit path length for the transition from the initial state i to the final state f with momentum $\vec{k}$ is given by [16] (atomic units are used in this paper unless otherwise stated):

$$\frac{\mathrm{d}P_{\mathrm{i}}^{(m)}(\vec{k}, z(x))}{\mathrm{d}\vec{k}\,\mathrm{d}x} = \delta_{\mathrm{S}} \int_{-\infty}^{+\infty} \mathrm{d}y\, P_{\mathrm{i}\vec{k}}^{(m)(\mathrm{at})}(\vec{\rho}(x,y)), \qquad (1)$$

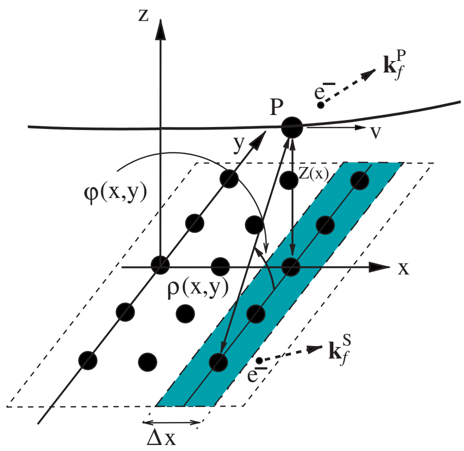

Fig. 1. Collision scheme.

where we denote with the upper index m = P, S the electrons ionized from the projectile and from the surface, respectively, $P_{\mathrm{i}\vec{k}}^{(\mathrm{m})(\mathrm{at})}(\vec{\rho})$ is the probability of atomic ionization depending on the impact-parameter $\vec{\rho}$ and δ_{S} is the surface atomic density which is considered as constant.

Thus, to obtain the final TDCS we first compute the ionization probability for both the projectile and the surface electrons for a given final state and then we integrate them over the classical trajectory taking into account the charge state of the projectile.

2.1. Projectile electrons

We assume that the projectile collides with the localized surface electrons. The differential cross section for H ionization by fast electrons in the projectile frame of reference is calculated in the impact parameter first Born approximation, being later referred to the laboratory system [6,17]. The hydrogenic electrons go from the Hydrogen fundamental state $|0\rangle$ to a Hydrogen continuum state with momentum $\vec{k}$ [13] and the surface electrons go from an initial state $|\mathrm{i}\rangle$ to a final state $|\mathrm{f}\rangle$. The transition amplitude for the binary collision under this assumptions is [11]:

$$A_{0\vec{k}}^{\mathrm{if}}(\vec{\rho}) = \left(\frac{-\mathrm{i}}{\pi v}\right) \int \frac{\mathrm{d}\vec{\eta}\, \exp(-\mathrm{i}\vec{\eta}\cdot\vec{\rho})}{\eta^2 + (\Delta E_{0k}^{\mathrm{if}}/v)} F_{0\vec{k}}(\vec{q}) G_{\mathrm{if}}(\vec{q}), \qquad (2)$$

where $\vec{\rho}$ is the collision impact parameter, $\vec{\eta}$ is the component of the transferred momentum $\vec{q}$ perpendicular to $\vec{v}_s$, $\Delta E_{0k}^{\rm if}$ is the target electron transition energy and $F_{0\vec{k}}(\vec{q})$ and $G_{\rm if}(\vec{q})$ are respectively the projectile and the target form factors [17].

Using closure approximation [7,8] we can take $\sum_{\rm f}|A_{0\vec{k}}^{\rm if}(\vec{\rho})|^2$ by $|\langle A_{0\vec{k}}(\vec{\rho})\rangle|^2$ and the target transition energy as

$$\Delta E_{0k}^{\rm if} \cong k^2/2 + 1/2 + q^2/2S(\vec{q}), \tag{3}$$

where $S(q)$ is the incoherent scattering function of the target atom [18].

Thus, for the transition probability of a projectile electron we have the expression:

$$P_{0\vec{k}}^{\rm (P)(at)}(\vec{\rho}) = |\langle A_{0\vec{k}}(\vec{\rho})\rangle|^2 = \left|\left(\frac{-{\rm i}}{\pi v}\right)\int \frac{{\rm d}\vec{\eta}\exp(-{\rm i}\vec{\eta}\cdot\vec{\rho})}{\eta^2+(\Delta E_{0k}^{\rm if}/v)} F_{0\vec{k}}(\vec{q})\sqrt{S(\vec{q})}\right|^2. \tag{4}$$

2.2. Surface electrons

To obtain the surface electron contribution we employ the CDW-EIS approximation to evaluate the atomic probabilities $P_{{\rm i}\vec{k}_{\rm f}}^{\rm (S)(at)}(\vec{\rho})$. The CDW-EIS T-matrix element reads:

$$T_{{\rm i}\vec{k}_{\rm f}}^{\rm CDW\text{-}EIS} = \langle \chi_{\rm f}^{\rm CDW}|W_{\rm f}^{\dagger}|\chi_{\rm i}^{E}\rangle, \tag{5}$$

where $\chi_{\rm f}^{\rm CDW}$ is the final CDW wave function, which contains a product of two continuum states, one around the target and the other around the projectile, $\chi_{\rm i}^{\rm E}$ is the Eikonal wave function and $W_{\rm f}$ is the final perturbative potential. In the CDW-EIS approximation the T-matrix element has a closed expression [14], and the atomic probability can be derived from Eq. (5) by using the well-known Eikonal transformation $P_{{\rm i}\vec{k}_{\rm f}}^{\rm (S)(at)}(\vec{\rho}) = |A_{{\rm i}\vec{k}_{\rm f}}^{\rm CDW\text{-}EIS}(\vec{\rho})|^2$ [11], where

$$A_{{\rm i}\vec{k}_{\rm f}}^{\rm CDW\text{-}EIS}(\vec{\rho}) = \frac{2\pi}{v_s}\int {\rm d}\vec{\eta}\, T_{{\rm i}\vec{k}_{\rm f}}^{\rm CDW\text{-}EIS}\exp({\rm i}\vec{\eta}\cdot\vec{\rho}) \tag{6}$$

is the CDW-EIS transition amplitude.

2.3. Projectile charge state

We are also interested in the projectile charge state, i.e. the projectile probability of being in either the ionized or the neutral state as a function of the height over the surface, $\phi_+(z)$ and $\phi_0(z)$ respectively.

In order to compute these we need to know, as a function of the height and per unit path, the probability of (i) the projectile being ionized from its neutral state, $P_{\rm loss}(z)$ and (ii) the projectile being neutralized from its ionized state, $P_{\rm capt}(z)$.

$P_{\rm loss}(z)$ is obtained just integrating the transition probability as a function of the impact parameter first over the strip normal to the projectile speed (Eq. (1)) and then over the ionized electron final momentum $\vec{k}$:

$$P_{\rm loss}(z) = \int {\rm d}\vec{k}\delta_{\rm S}\int_{-\infty}^{+\infty} {\rm d}y P_{0\vec{k}}^{\rm (P)(at)}(\vec{\rho}(x,y)). \tag{7}$$

To evaluate $P_{\rm capt}(z)$ we employ the prior version of the Eikonal-impulse approximation, which is a distorted wave method making use of the exact impulse and Eikonal wave functions in the final and initial channels respectively [19,20].

Fig. 2 shows the results obtained for a LiF surface (see Section 3 for a complete description of the system). The projectile loss probability is, for every distance to the surface, at least one order or magnitude greater than the capture probability. Accordingly we will find that the projectile is in its ionized state along most of the collision path.

To account for the projectile trajectory we use the relation ${\rm d}x/{\rm d}z = v_s/v_z(z)$:

$$\frac{{\rm d}P_{\rm if}}{{\rm d}z} = \frac{v_s}{v_z(z)}\frac{{\rm d}P_{\rm if}}{{\rm d}x}, \tag{8}$$

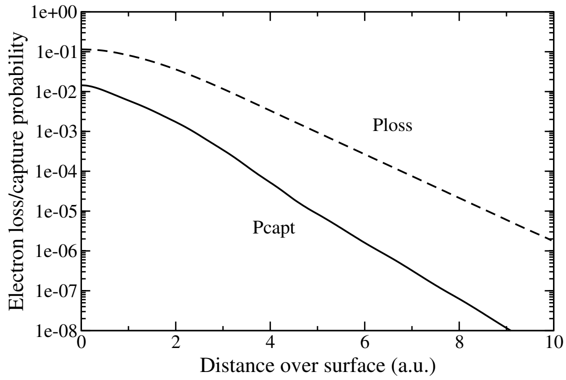

Fig. 2. $P_{\rm loss}$ and $P_{\rm capt}$ for LiF surface.

with $z(x)$ being the parameterized trajectory, obtained assuming a ZBL [21] planar potential for the surface–proton interaction.

The probabilities for the projectile to be in its neutral or ionized states are given by the set of differential equations

$$\frac{d\phi_+(z)}{dz} = \phi_0(z)\frac{v_s}{v_z(z)}P_{\mathrm{loss}}(z) - \phi_+(z)\frac{v_s}{v_z(z)}P_{\mathrm{capt}}(z) \tag{9}$$

and

$$\frac{d\phi_0(z)}{dz} = \phi_+(z)\frac{v_s}{v_z(z)}P_{\mathrm{capt}}(z) - \phi_0(z)\frac{v_s}{v_z(z)}P_{\mathrm{loss}}(z), \tag{10}$$

where both probabilities satisfy the equation

$$\phi_0(z) + \phi_+(z) = 1 \tag{11}$$

and the boundary condition is $\phi_0(-\infty) = 0$ as the surface is impinged with a proton beam.

In Fig. 3 we can see that up to 5 a.u. from the surface the projectile maintains its initial ionized state from where it gets a higher chance of being in the neutral state up to a maximum probability of about 9% at the trajectory turning point at 0.54 a.u.

2.4. Final emission

For a given height over the surface and a final electron momentum, we compute both the surface and projectile emission probabilities and the charge state of the projectile. By weighting the former with the latter we obtain the electron emission probability

$$\frac{dP^4(\vec{k}_f, z)}{d\vec{k}\,dz} = \phi_0(z)\frac{v_s}{v_z(z)}\frac{dP_i^{(P)}(\vec{k}_f, z)}{d\vec{k}\,dx} + \phi_+(z)\frac{v_s}{v_z(z)}\frac{dP_i^{(S)}(\vec{k}_f, z)}{d\vec{k}\,dx}. \tag{12}$$

Integrating over the projectile trajectory we obtain the triple differential cross section for the electron emission

$$\frac{d^3P(\vec{k}_f)}{d\vec{k}} = \int_{z\in\mathrm{trajectory}} dz\frac{d^4P(\vec{k}_f, z)}{d\vec{k}\,dz}. \tag{13}$$

3. Results

The system considered consists of a proton moving with an initial trajectory of 0.7° against a LiF(0 0 1) surface. The proton velocity is 2 a.u. and the trajectory it follows is given by a ZBL surface–proton planar potential.

For this system we compute the electron emission cross section for different polar angles in the scattering plane as a function of the emitted electron energy, the polar angle being referred to the surface. The results obtained for polar angles of 0.7°, 5.0°, 10.0° and 20.0° are shown in Fig. 4.

As we increase the polar angle from 0.7° to 20° the convoy peak decreases its magnitude by almost two orders of magnitude and shifts by about 10 eV towards lower energy while its width increases. At 20° the peak can still be discerned, although quite softened.

The ELC electrons, which are mainly emitted isotropically around the ionization threshold in the projectile frame of reference, become highly localized at low polar angles when changing to the laboratory frame of reference. The peak position, E_p, for a given polar angle θ_i, is approximately given by $E_p \simeq k_p^2/2$, with $k_p = k\cos\theta_i$.

This shift is in agreement with experimental observation [2]. However, the intensity of the peak as a function of the angle of emission decreases

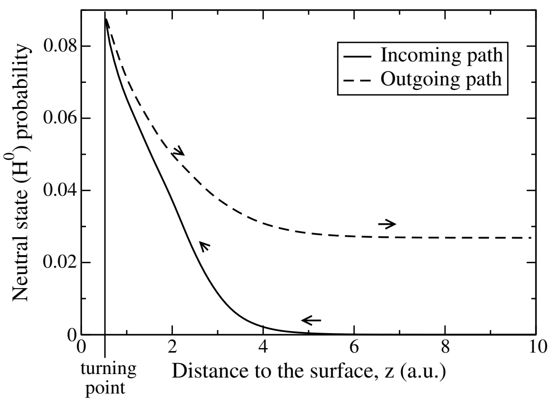

Fig. 3. Probability of the projectile being in the neutral state as a function of the height over the LiF surface.

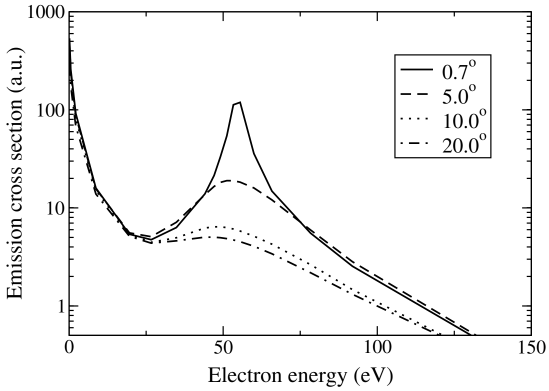

Fig. 4. Electron emission cross section for different polar angles.

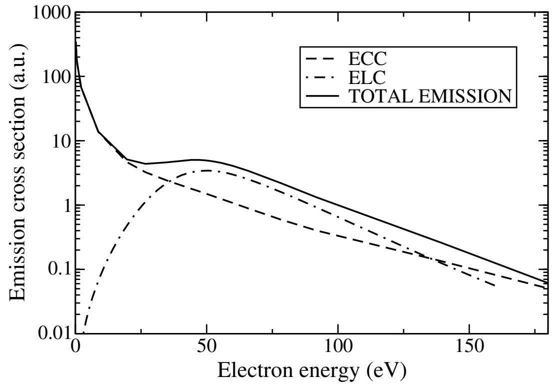

Fig. 6. H^+–LiF electron emission at 20° polar angle; projectile (dashed line) and surface (dash-dotted line) electron contributions.

much faster in our model than in the experiments as we have not only used a perturbative approach but also a simple model for the target electrons.

The individual contribution from the ELC and ECC electrons is shown in Figs. 5 and 6 for emission angles of 0.7° and 20° respectively. At low electron energies only the surface electrons contribute to the TDCS, while at the convoy peak energies a different behavior occurs. For the lower angle of emission we see that both contributions to the convoy electrons are quite similar, not being so at the higher angle, where the ECC electrons do not show any structure at convoy energies.

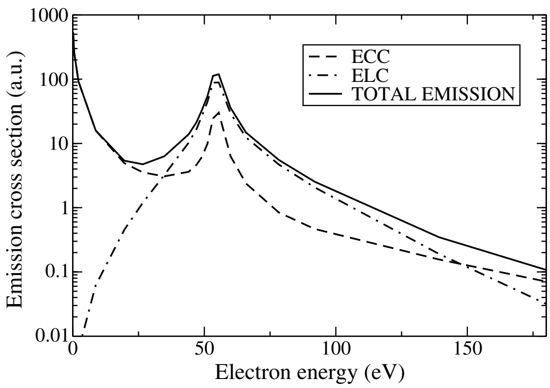

Fig. 5. H^+–LiF electron emission at 0.7° polar angle; projectile (dashed line) and surface (dash-dotted line) electron contributions.

4. Conclusions

The model described for the H^+–LiF grazing collision electron emission shows that the projectile electron contribution to the total emission is of the order, or even greater than, the surface electrons, at convoy peak energies. At polar angles of emission $\gtrsim$ 15° in the scattering plane the contribution of the surface electrons to the convoy electrons becomes negligible, being the peak formed mostly by projectile electrons.

Acknowledgments

This work was in part supported by Eusko Jaurlaritza, Euskal Herriko Unibertsitatia, Donostia International Physics Center and the Spanish MCYT (under contract BFM2001-0076).

References

[1] K. Kimura, M. Tsuji, M. Hiko Mannami, Phys. Rev. A 46 (5) (1992) 2618.
[2] E. Sanchez, O. Grizzi, G. Nadal, G. Gómez, M. Martiarena, V. Ponce, Nucl. Instr. and Meth. B 90 (1994) 261.
[3] M. Martiarena, E. Sánchez, O. Grizzi, V. Ponce, Phys. Rev. A 53 (2) (1996) 895.
[4] K. Kimura, G. Andou, K. Nakajima, Nucl. Instr. and Meth. B 164–165 (2000) 933.
[5] H. Winter, Phys. Rep. 367 (2002) 387.

[6] J. Briggs, F. Drepper, J. Phys. B 23 (23) (1978) 4033.
[7] Y.T. Lee, J.C. Chen, Phys. Rev. A 19 (2) (1979) 526.
[8] V. Ponce, R. Baragiola, J. Phys. B 17 (1984) 2467.
[9] A. Salin, J. Phys. B 22 (1989) 3901.
[10] R. McCarroll, A. Salin, J. Phys. B 1 (1968) 163.
[11] M. McDowell, J.P. Coleman, Introduction to the Theory of Ion–atom Collisions, North-Holland, Amsterdam, 1970.
[12] M.L. Martiarena, V.H. Ponce, Nucl. Instr. and Meth. B 203 (2003) 62.
[13] L. Landau, E. Lifschitz, Quantum Mechanics, Pergamon, Oxford, 1977.
[14] P. Fainstein, V. Ponce, R. Rivarola, J. Phys. B 22 (1989) 1207.
[15] P. Fainstein, V. Ponce, R. Rivarola, J. Phys. B 24 (1991) 3091.
[16] M. Gravielle, Phys. Rev. A 62 (2000) 062903.
[17] I. Aldazabal, V. Ponce, A. Arnau, Phys. Status Solidi (b) 241 (10) (2004) 2374.
[18] J. Hubbell et al., J. Phys. Chem. Ref. Data 4 (3) (1975) 471.
[19] M. Gravielle, J. Miraglia, Phys. Rev. A 44 (1991) 7299.
[20] M. Gravielle, J. Miraglia, Phys. Rev. A 51 (1995) 2131.
[21] J. Ziegler, J. Biersack, U. Littmark, The Stopping and Range of Ions in Matter, vol. 1, Pergamon, New York, 1985.